Popular Summary

Deforestation is rapidly increasing in Amazonia. If deforestation continues at the current rate, most of the Amazonian tropical forests would disappear in less than 100 years. One question that arises is whether large-scale deforestation in Amazonia might affect the regional climate. Early modeling studies concluded that widespread deforestation of Amazonia would lead to decreased rainfall. More realistic and sophisticated mesoscale models show that deforestation can create localized circulations with rising motions over the deforested areas. The potential impact of these circulations on cloudiness and rainfall is the subject of this paper. We analyze geosynchronous (GOES) infrared satellite data with respect to cloudiness, and analyze passive microwave data from sensors aboard the Tropical Rainfall Measuring Mission satellite with respect to rainfall. We conclude that in the dry-season (August) when the effects of the surface are not overwhelmed by large-scale weather disturbances, the occurrence of cloudiness and rainfall increase over the deforested and non-forested (savanna) regions. During the day, the amount of cloudiness shifts toward afternoon hours in the deforested and savanna regions, as compared to the forested regions. Analysis of 14 years of monthly estimates from the Special Sensor Microwave/Imager revealed that only in August did rainfall amounts increase over the deforested region.

The Impact of Amazonian Deforestation on Dry-Season Rainfall

Andrew J. Negri, Robert F. Adler
Laboratory for Atmospheres
NASA/Goddard Space Flight Center, Greenbelt, MD 20771

Liming Xu
Department of Hydrology and Water Resources
University of Arizona, Tucson, AZ 85721
and

Jason Surratt
Department of Marine, Earth and Atmospheric Sciences
North Carolina State University 27606

Draft for submission to Science
5/6/02

The Impact of Amazonian Deforestation on Dry-Season Rainfall

Andrew J. Negri[1*], Robert F. Adler[1], Liming Xu[1,2], and Jason Surratt[3]

Many modeling studies have concluded that widespread deforestation of Amazonia would lead to decreased rainfall. We analyze geosynchronous infrared satellite data with respect percent cloudiness, and analyze rain estimates from microwave sensors aboard the Tropical Rainfall Measuring Mission satellite. We conclude that in the dry-season, when the effects of the surface are not overwhelmed by synoptic-scale weather disturbances, deep convective cloudiness, as well as rainfall occurrence, all increase over the deforested and non-forested (savanna) regions. This is in response to a local circulation initiated by the differential heating of the region's varying forestation. Analysis of the diurnal cycle of cloudiness reveals a shift toward afternoon hours in the deforested and savanna regions, compared to the forested regions. Analysis of 14 years of data from the Special Sensor Microwave/Imager data revealed that only in August did rainfall amounts increase over the deforested region.

[1] Laboratory for Atmospheres, NASA/Goddard Space Flight Center, Greenbelt, MD 20771

[2] Department of Hydrology and Water Resources, University of Arizona, Tucson, AZ 85721

[3] Department of Marine, Earth and Atmospheric Sciences, North Carolina State University 27606

[*] To whom correspondence should be addressed. E-mail: negri@agnes.gsfc.nasa.gov

The objectives of this study are to demonstrate that in the dry season, increased surface heating over deforested regions creates a direct thermal circulation, which increases the occurrence of both deep convective cloudiness and rainfall. Similar (and more pronounced) effects are noted over a small, naturally unforested region of savanna, suggesting that size or scale may play a role in modulating the resultant circulation.

Initial modeling efforts assumed widespread Amazonian deforestation. Simulations using a global spectral model found that large-scale conversion of forest to pasture decreased the precipitation 25% (1). Using the Goddard Global Circulation Model (GCM), a 5-day simulation showed a decrease in precipitation of 8% in the wettest month of the year (2). The NCAR community climate model results noted a shift in wet season precipitation with deforestation rather than an overall decrease over the deforested area (3). More recent modeling work utilized a mesoscale model with realistic forcing using a "fish-bone" pattern (4). This revealed that mesoscale circulations enhanced cloudiness and localized rainfall as well as dry season enhancement of shallow clouds under weak synoptic forcing. Observations and modeling of landscape heterogeneity resulting from differential land use indicated a direct thermal circulation over the Midwest (5).

Observations have not borne out the initial modeling studies. Analysis of Outgoing Longwave Radiation (OLR) from 1974-90 and monthly rainfall at Belem and Manaus, both showed upward trends in cloudiness and precipitation, despite deforestation in that period (6). Using the Global Historical Climatological Network (GHCN) [7], OLR and National Centers for Environmental Prediction (NCEP) reanalysis, an increasing rainfall trend over Amazon Basin due to global divergent circulation was noted (8). It was postulated that this global circulation suppresses the full impact of deforestation. When the dry season in particular was examined, higher temperatures, higher sensible heat flux, and deeper convective boundary layers over the deforestation were found (9). Using Geosynchronous Operational Environmental Satellite (GOES) visible imagery, an enhanced frequency of shallow cumulus cloud where forest was cleared was observed (10). Increased surface temperature in deforested regions has been observed (11). Tropical Rain Measuring Mission (TRMM) data have revealed an average increase of 28% downwind of urban metropolis (12), also the result of artificially induced mesoscale circulations.

Figure 1 displays a highly enhanced, 1 km resolution, cloud-free GOES visible channel image of the area of study at 1130 LT on 8 Aug 2001 (13). Brighter shading represents areas of deforestation, with the exception of a naturally unforested region of savanna in the northeast. Deforestation is evident along roads and waterways, and the "fish-bone" pattern modeled by Wang et al (4) is clearly evident. Grid squares (0.5° resolution) have been characterized by visible brightness, as deforested (D), forested (F), and mixed (M). An additional, subjective determination resulted in five grid cells classified as savanna (S).

Figure 2 shows a composite of GOES infrared-derived surface temperatures (under clear-sky conditions) for 1230 LT during August 2000. Outlines of the visible deforestation from Fig. 1 are superimposed. Increased surface heating is evident over the deforested and savanna area, on the order of 5-10 K. This has also been observed from METEOSAT observations (11) and from in-situ measurements (9).

The occurrence of deep convection can be represented by the fractional occurrence of cloud colder than 225 K. Figures 3 and 4 display the fractional coverage of cold cloud as measured by the GOES IR sensor for August 2000/01 and September 2000/01 respectively. To ensure frequent and consistent sampling, the 30-min interval GOES data has been accumulated into three 8-h periods, plus a 24-h total. The impact of deforestation on the cloud amount is most pronounced in August (Fig. 3) in the period 12-19 LT. Interestingly, two other areas to the north of the main area of deforestation also appear to spawn frequent convection. One area is the inverted V-shaped savanna region identified in Fig 1. The other is an inverted V-shaped region of deforestation to the west, along a (presumably) dry riverbed. These two areas spawn convection at twice the frequency of the larger deforested region. In September (Fig. 4) the aforementioned two areas are also active regions of convection (almost 20% of the time period 12-19 LT). The effects of the main deforestation area are apparent in the increased cloud cover at both 12-19 and 20-03 LT.

It is hypothesized that the differential heating across these regions of deforestation and naturally occurring savanna creates a local, direct circulation, which increases the cloudiness over these regions. Prevailing easterly flow may actually shift the center of convergence towards the east in September.

A word about topography: the region is at the southern extent of the Amazon "Basin". While the northern portion of the region is flat and under 100m in elevation, there is a ridge of higher land (300-700 m) that runs WNW to SSE across the southern portion of the area. Easterly flow across the region could force some cloudiness along this ridge,

which might account for some of the effects we attribute to the circulations induced by differential surface characteristics.

To accumulate enough sampling to adequately describe the diurnal cycle, we combine the cloudiness data for Aug and Sep 2000/2001. Figure 5 displays a time series of the mean IR cloudiness for various surface types, as characterized in Fig. 1. The surface type with the highest amplitude diurnal signal is the savanna, peaking at 16 LT. Of interest is the difference between the diurnal signals for the forested (green) and deforested (orange) curves. The percent cold cloudiness is slightly higher in the forested regions from 03 LT until 1530, after which the deforested regions have a higher percent cloudiness. Times at which the difference in these means is significant at the 0.05 (or less) level are indicated by an "s" along the top. Sampling (maximum of 122 days) is also indicated along the top of the figure.

Data from the TRMM were analyzed for the percent occurrence of rain for the periods matching Figs 3 and 4. TRMM is in a 35°-inclination orbit and precesses through the diurnal cycle every 46 days. Rainrates are produced by the application of the Goddard Profiling (GPROF) [14,15] to the TRMM Microwave Instrument (TMI). Orbit data at 0.1° resolution were analyzed the occurrence of non-zero rainrates (16). Results are shown in Figures 6 and 7. Results for August 2000/2001 (Fig. 6) confirm the IR results of Fig 3; i.e. increased occurrence of rainfall over the savanna, over the deforested strip to it's west and over the center of the main area of deforestation, in the period 12-19 LT. Results for September (Fig. 7) indicate an increased probability of rain over the deforestation during the period 20-03LT. The preferred region of rainfall occurrence is just southwest of the savanna at 12-19 LT.

For a longer record we examine data from the Special Sensor Microwave Imager (SSM/I), using data from the series of sun-synchronous satellites that have overpasses at 06/18 LT. The SSM/I provides about 40 samples per month over this region. Figure 8 shows the results of the mean GPROF-derived rainrate for the 14-year period of record. The only month to show an increase in rainrate over the deforested area was August (top). September (bottom) for example, actually has a rainrate minimum over this region.

Analysis of long-term *in-situ* precipitation from the GHCN (7) is inconclusive, due to both the low rain amounts during this period, and the absence of gages outside of the deforested regions.

The scenario presented here, based on satellite observations of cloudiness and rainfall, is in agreement with the most recent and sophisticated mesoscale models. These conclude

that mesoscale circulations induced by heterogeneous land surface could enhance cloudiness and local rainfall (4). The effects are most pronounced in August, during the transition from dry to wet season.

References and Notes

1. C. A. Nobre, P. J. Sellers, J. Shukla, *J. Clim.* **4**, 957 (1991).
2. G. K. Walker, Y. C. Sud, R. Atlas, *Bull. Amer. Meteor. Soc.* **76**, 346 (1995).
3. A. N. Hahmann, R. E. Dickinson, *J. Clim.* **10**, 1944 (1997).
4. J. Wang, R. L. Bras, E. A. B. Eltahir, *J. Hydromet.* **1**, 267 (2000).
5. C. P. Weaver, R. Avissar, *Bull. Amer. Meteor. Soc.* **82**, 269 (2001).
6. P-S. Chu, Z-P. Yu, S. Hastenrath, *Bull. Amer. Meteor. Soc.* **75**, 579 (1994).
7. D. R. Easterling, T. C. Peterson, T. R. Karl, *J. Clim.* **9**, 1429 (1996).
8. T-C. Chen, J-H. Yoon, K. J. St. Croix, E. S. Takle, *Bull. Amer. Meteor. Soc.* **82**, 2209 (2001).
9. J. H. C. Gash, C. A. Nobre, *Bull. Amer. Meteor. Soc.* **78**, 823 (1997).
10. E. Cutrim, D. W. Martin, R. Rabin, *Bull. Amer. Meteor. Soc.* **76**, 1801 (1995).
11. J-C. Calvert *et al.*, *Bull. Amer. Meteor. Soc.* **78**, 413 (1997).
12. J. M. Shepherd, H. Pierce, A. J. Negri, *J. Appl. Meteor.* **41**, 1853 (2002).
13. GOES-east begins scanning at 15 and 45 minutes past the hour, and scans the study area about 15 min later. The study area is four hours earlier than GMT.
14. C. D. Kummerow, L. Giglio, *J. Appl. Met.* **33,** 3 (1994).
15. C. D. Kummerow *et al.*, *J. Appl. Met.* **39,** 1965 (2000).
16. A note on sampling: the TMI, with observations aggregated over an 8-h period, will sample a two-month period about 15-25 times. [17].
17. A. J. Negri, T. L. Bell, L. Xu, *J. Atmos. Ocean. Tech.* **19**, in press (2002).

18. The authors acknowledge the support of NASA's Atmospheric Dynamics and Remote Sensing Program, Dr. Ramesh Kakar, Manager.

Figure Captions

Fig. 1. Enhanced GOES 1 km visible image at 1130 LT 08 Aug. 2001 over a heavily deforested region of Rondonia, Brazil. Classification of 0.5° grid boxes is; F (forested); D (Deforested), S (Savanna) and M (Mixed).

Fig. 2. GOES 4 km infrared composite mean (clear-sky) temperatures at 1230 LT for August 2000.

Fig. 3. Percent occurrence of cold (225K) cloudiness from GOES 4 km infrared data for August 2000/2001. Half-hourly GOES data have been composited into three 8-h periods and a 24-h composite.

Fig. 4. Same as Fig.3 except September 2000/2001.

Fig. 5. Time series of the mean percent cloudiness data for August-September 2000/2001 stratified into the four indicated surface types. Plotted across the top is the number of samples (maximum of 122). The significance level (<0.05) of the difference in the mean percent cloudiness between the forested and deforested points is denoted by an "s".

Fig. 6. Percent occurrence of rain at 0.1° resolution derived from the application of the GPROF algorithm to data from the TRMM Microwave Imager. Data are from August 2000/2001 and are composited as in Fig. 3.

Fig. 7. As in Fig. 6 except September 2000/2001

Fig. 8. Rainrate (mm/h) at 0.5° resolution derived from the application of the GPROF algorithm to data from the Special Sensor Microwave/Imager overpasses at 06/18 LT. August (top) and September (bottom) 1987-2001

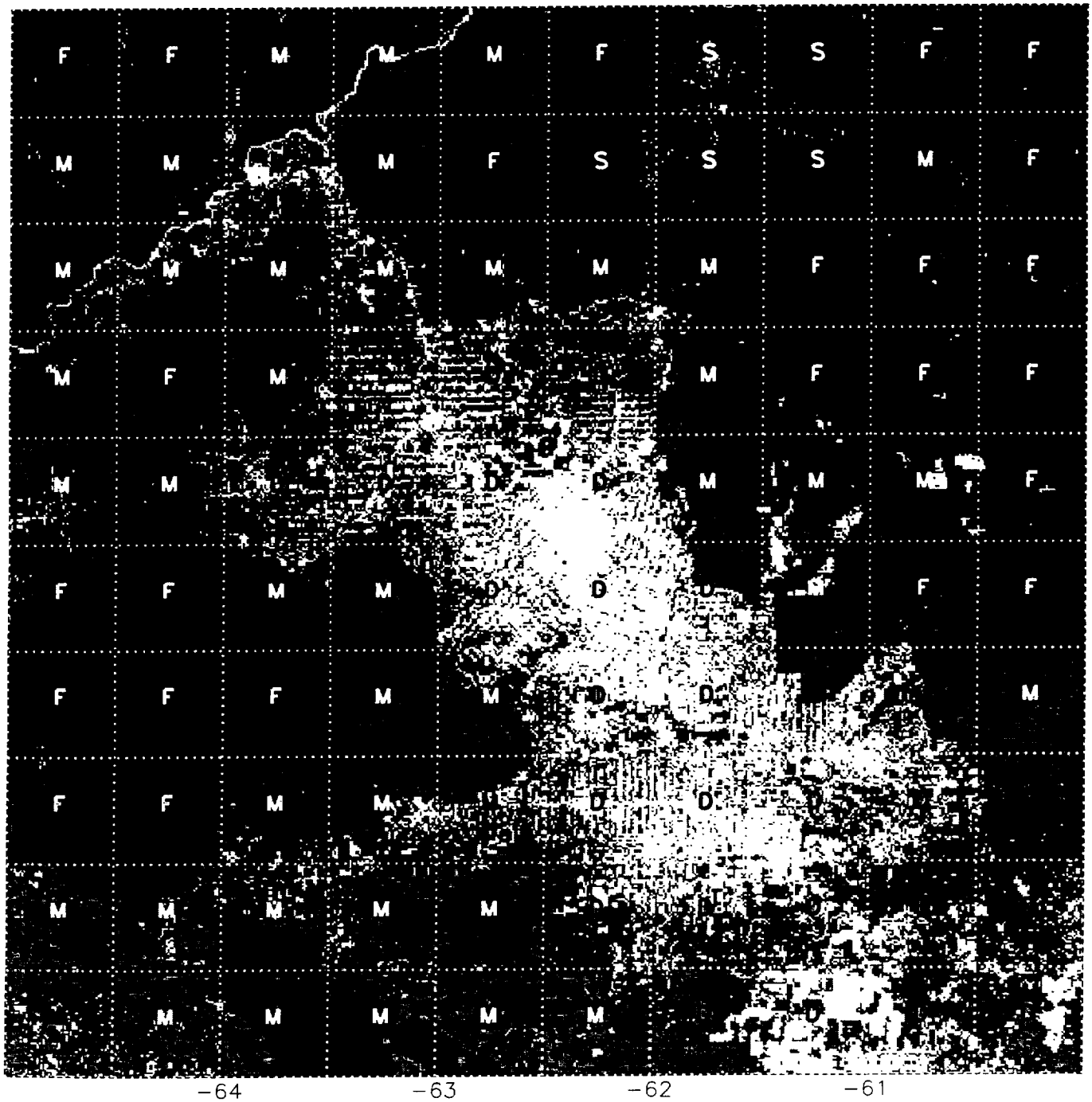
F F M M M F S S F F
M M M F S S S M F
M M M M M M M F F F
M F M M F F F
M M D D M M M F
F F M M D D D F F
F F F M M D D M
F F M M D D
M M M M M D
M M M M M D
−9
−10
−11
−12
−64
−63
−62
−61

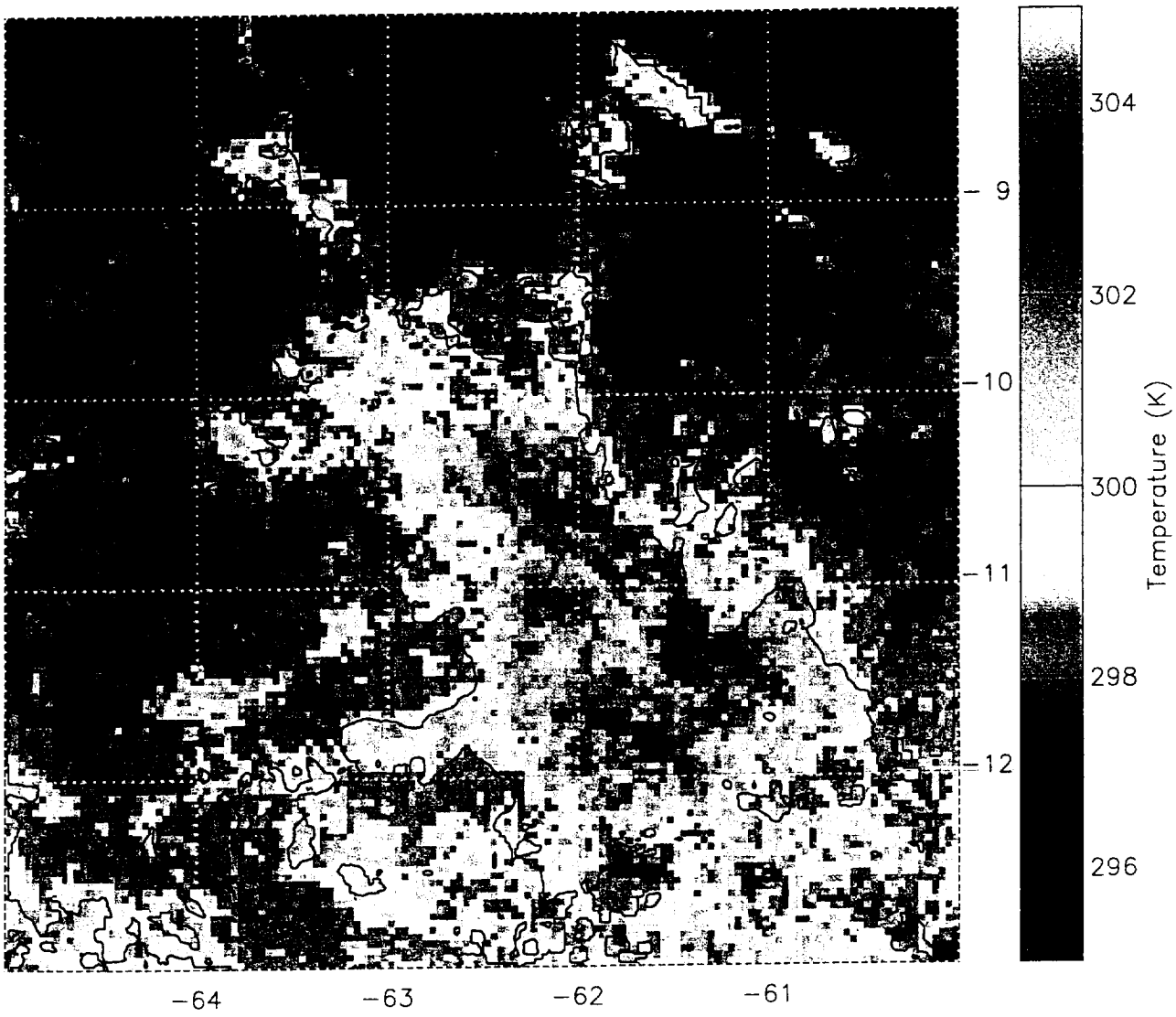
−9
−10
−11
−12
−64
−63
−62
−61
304
302
300
298
296
Temperature (K)

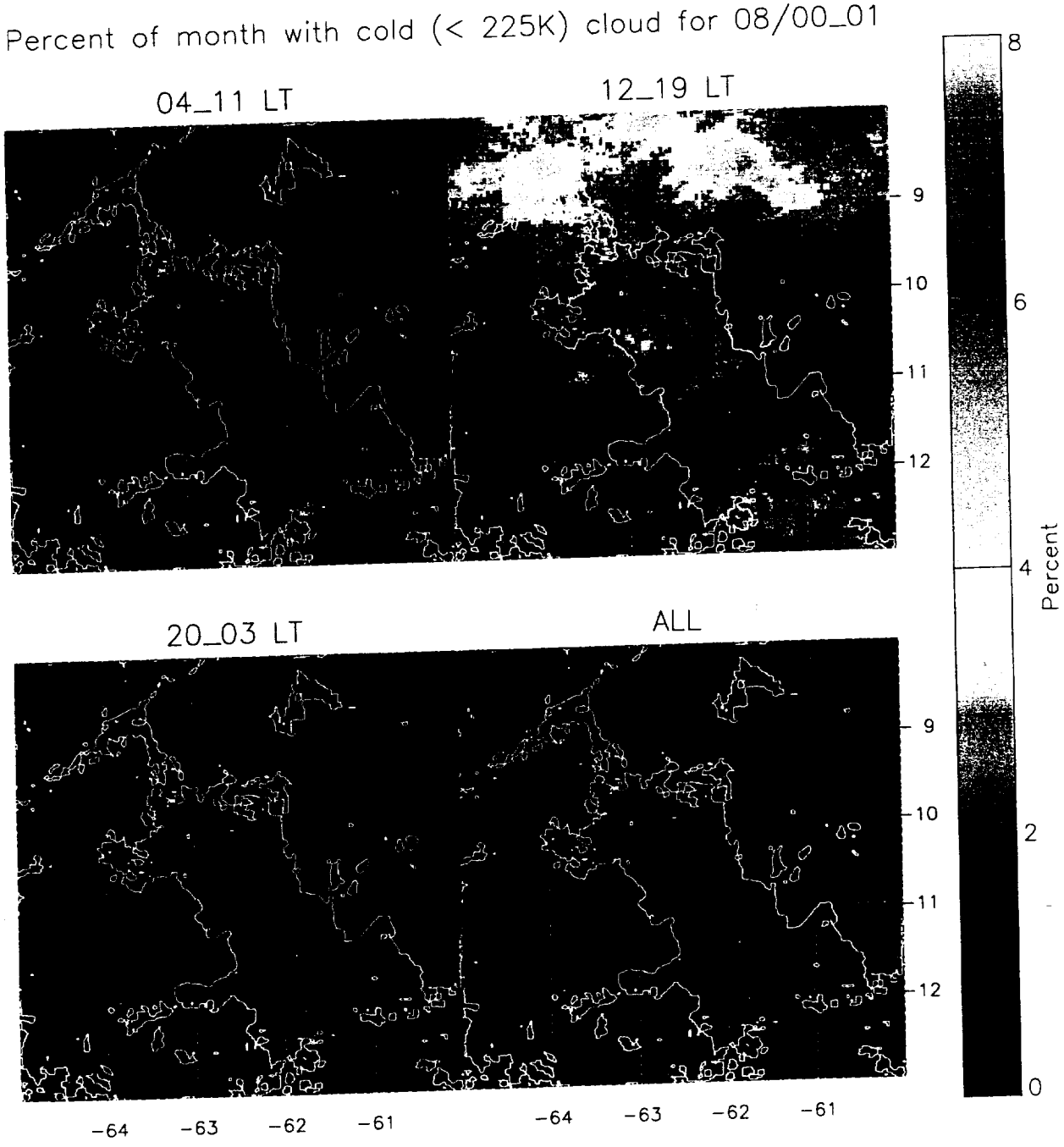
Percent of month with cold (< 225K) cloud for 08/00_01
04_11 LT
12_19 LT
20_03 LT
ALL
9
10
11
12
-64
-63
-62
-61
8
6
4
2
0
Percent

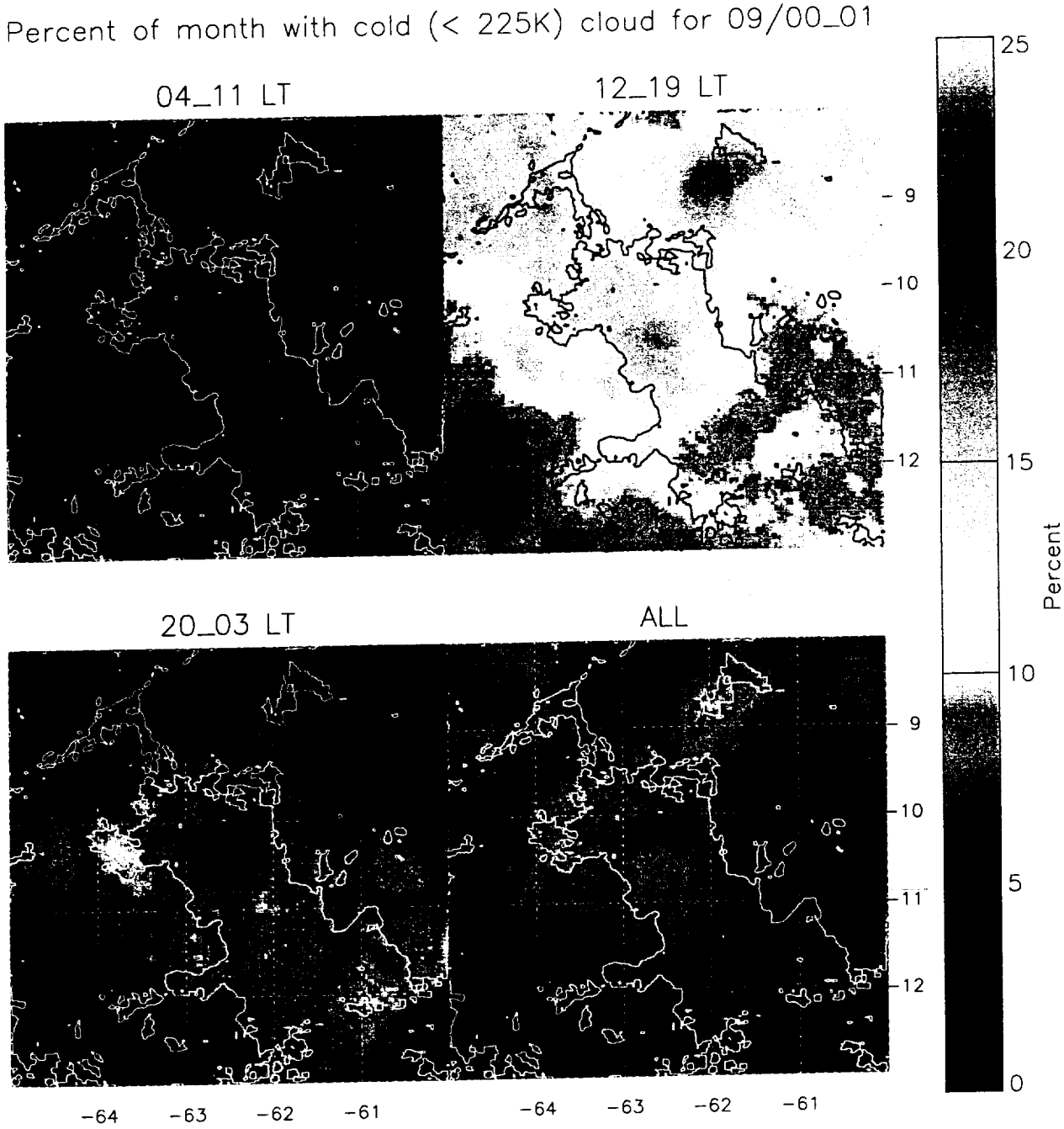
Percent of month with cold (< 225K) cloud for 09/00_01
04_11 LT
12_19 LT
20_03 LT
ALL
-9
-10
-11
-12
-64
-63
-62
-61
25
20
15
10
5
0
Percent

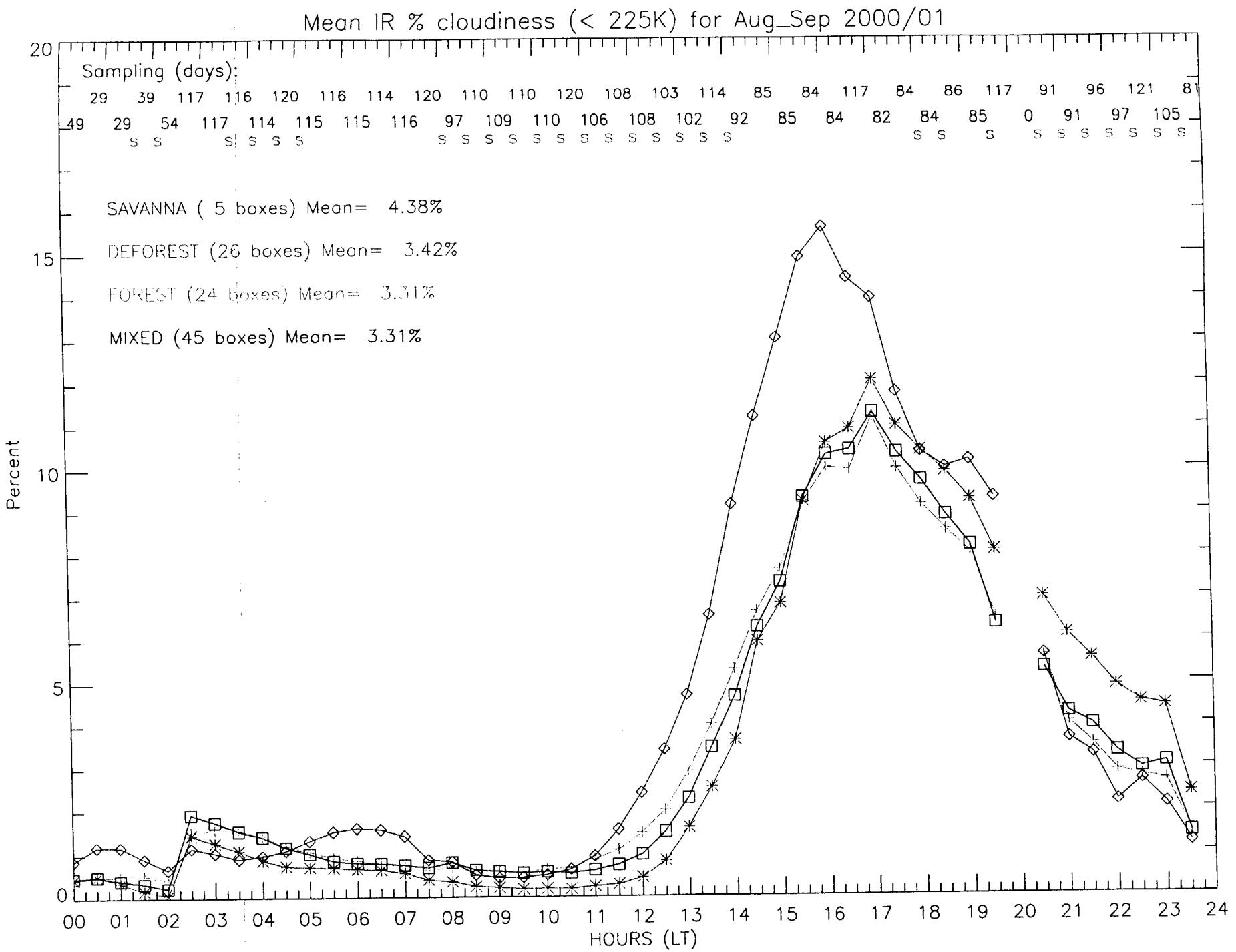
Mean IR % cloudiness (< 225K) for Aug_Sep 2000/01
Sampling (days):
29 39 117 116 120 116 114 120 110 110 120 108 103 114 85 84 117 84 86 117 91 96 121 81
49 29 54 117 114 115 115 116 97 109 110 106 108 102 92 85 84 82 84 85 0 91 97 105
SAVANNA (5 boxes) Mean= 4.38%
DEFOREST (26 boxes) Mean= 3.42%
FOREST (24 boxes) Mean= 3.31%
MIXED (45 boxes) Mean= 3.31%
Percent
HOURS (LT)
0
5
10
15
20
00 01 02 03 04 05 06 07 08 09 10 11 12 13 14 15 16 17 18 19 20 21 22 23 24

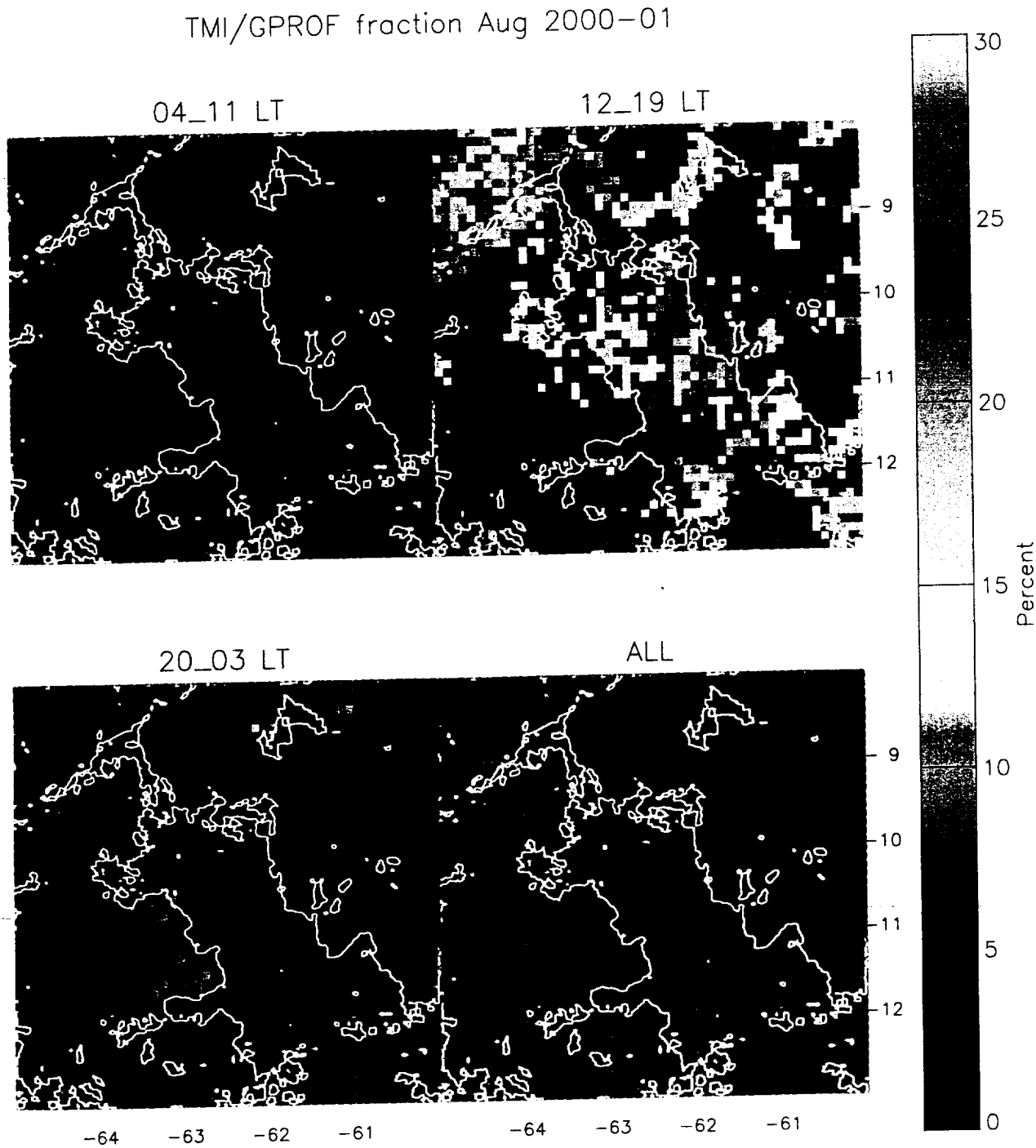
TMI/GPROF fraction Aug 2000-01
04_11 LT
12_19 LT
20_03 LT
ALL
9
10
11
12
-64
-63
-62
-61
30
25
20
15
10
5
0
Percent

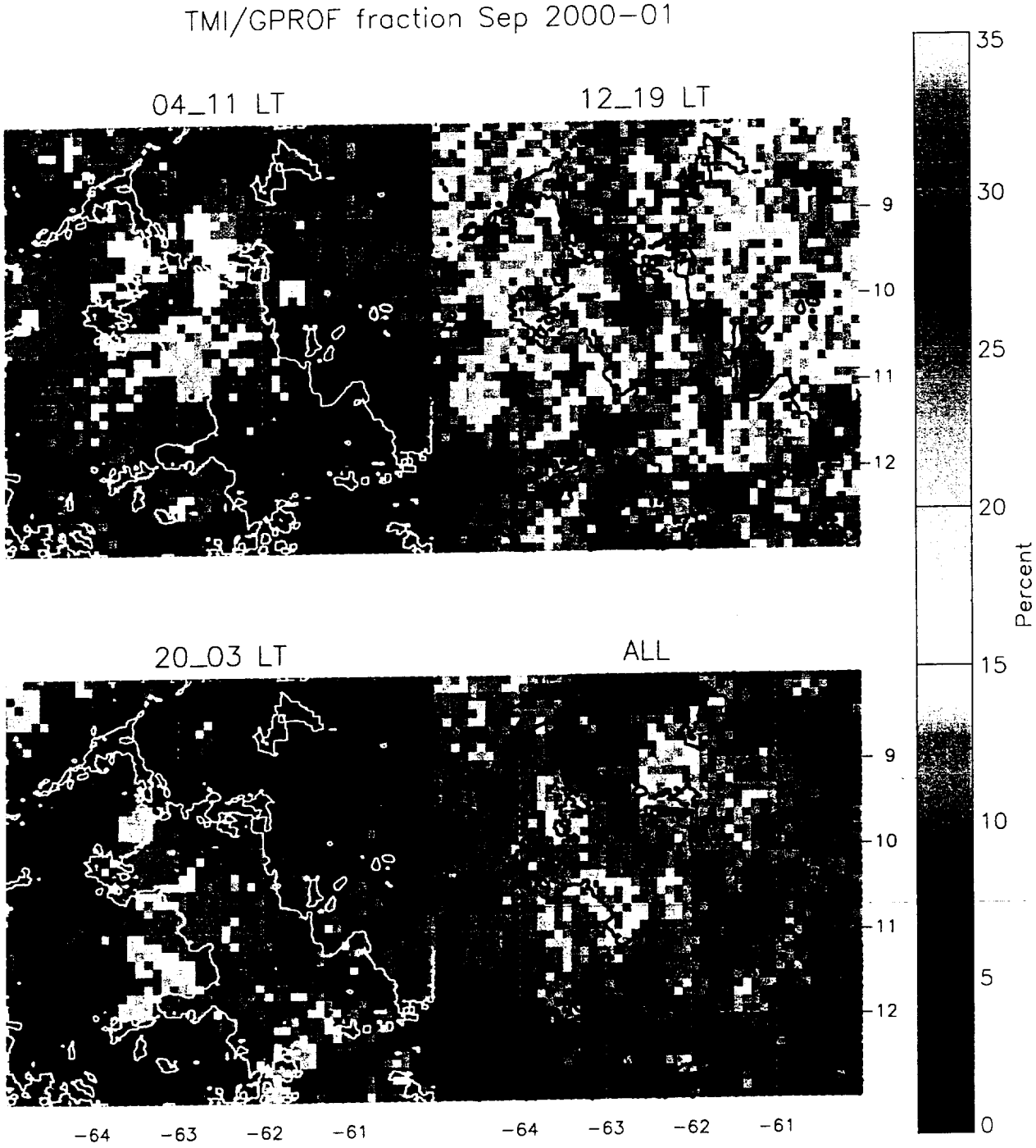
TMI/GPROF fraction Sep 2000–01
04_11 LT
12_19 LT
20_03 LT
ALL
9
10
11
12
−64
−63
−62
−61
35
30
25
20
15
10
5
0
Percent

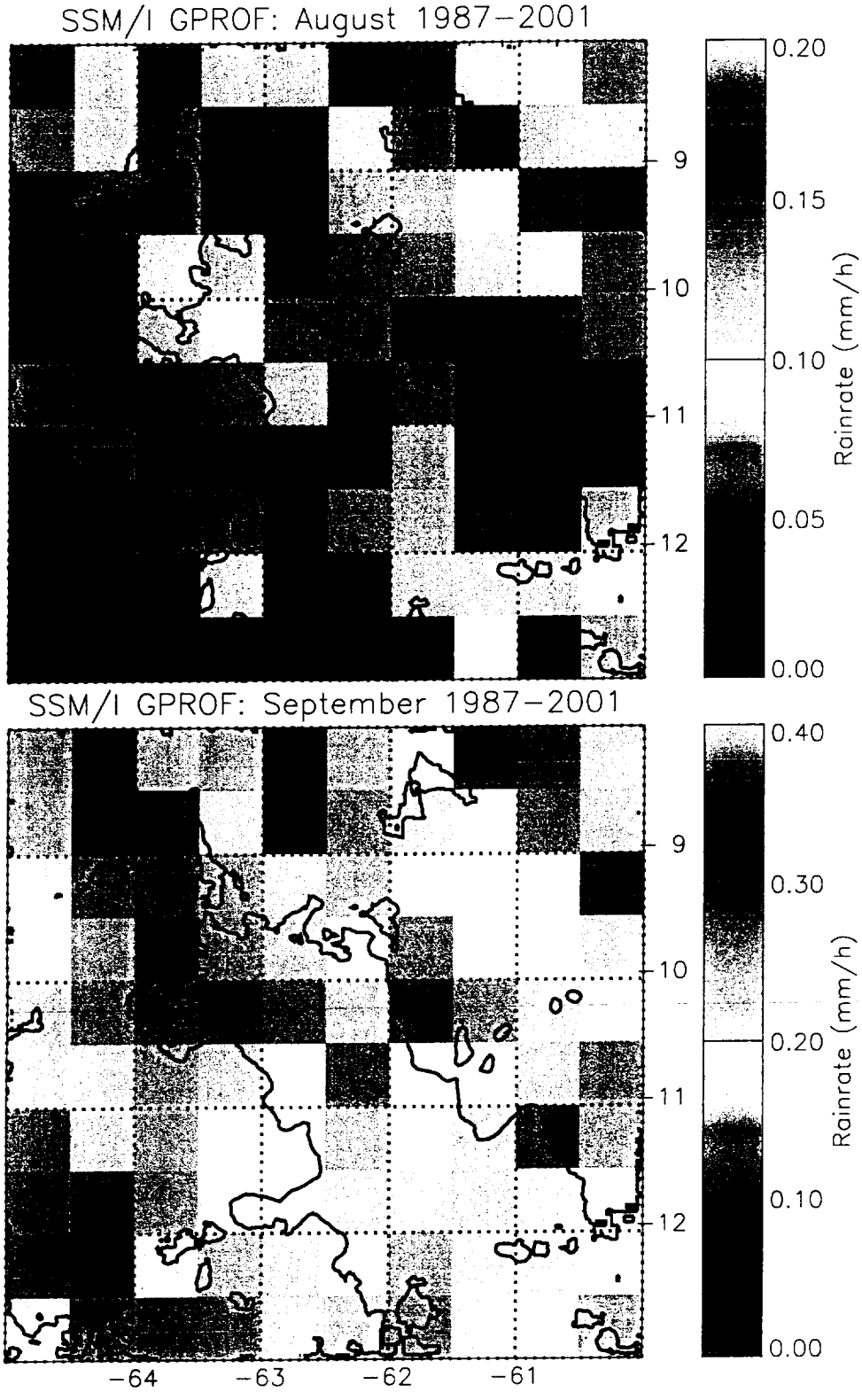
SSM/I GPROF: August 1987–2001
9
10
11
12
0.20
0.15
0.10
0.05
0.00
Rainrate (mm/h)
SSM/I GPROF: September 1987–2001
9
10
11
12
0.40
0.30
0.20
0.10
0.00
Rainrate (mm/h)
−64
−63
−62
−61